Available online at www.sciencedirect.com
SCIENCE DIRECT
Catalysis Today 105 (2005) 499–506
CATALYSIS TODAY
www.elsevier.com/locate/cattod

New TiO_2 monolithic supports based on the improvement of the porosity

S. Suárez, M. Yates, P. Avila, J. Blanco *

Instituto de Catálisis y Petroleoquímica, C/Marie Curie no. 2, Cantoblanco, Madrid 28049, Spain

This article is dedicated to the memory of Dr. Paul Grange and Dr. Ricardo Linarte.

Abstract

Titania monolithic supports produced with an additional macroporosity were prepared and their behaviour compared with commercial materials of the same composition. Activated carbon used as a template for macropore generation, was included in the preparation process of the ceramic dough. Mercury intrusion porosimetry (MIP), nitrogen adsorption–desorption, X-ray diffraction (XRD), TGA–DSC analyses were employed to study the modifications of the support properties. The systems prepared with the template, which was subsequently eliminated by thermal treatment, presented a notable increase in the macropore volume with respect to samples prepared without this pore generating agent (PGA), displaying a narrow pore size distribution with a mean pore diameter of 0.13 μm. The template was chemically inert and no modification on the crystal phases or the BET area was observed. The optimum composition was achieved for a sample produced with 10 wt.% of template and subsequently heat-treated in air at 550 °C to remove the PGA. Vanadia catalysts based on these supports displayed higher NO_x conversions during the NO and NO_x elimination by the SCR process at low temperature than the standard ones. This behaviour was related to the improvement in the effectiveness factor due to the reduction of the internal mass transfer limitations.

Keywords: Monoliths; Activated carbon; Pore generating agent (PGA); Titania supports; Macroporosity; Effectiveness factor; SCR process

1. Introduction

From the first studies in the fifties the use of monoliths or honeycomb catalysts [1] has experienced an exponential growth [2–4]. Besides their applications within environmental scenarios their employment in various processes such as hydrotreatment (HDS, HDN), catalytic combustion, Fischer Tropsch synthesis, biology, electrochemistry, is currently under study [5–8]. Compared to conventional structured catalysts (spheres, cylinders, rings, extrudates) monolithic structures present attractive advantages for industrial applications, among which should be mentioned their low pressure drop, high surface area, the ability to treat large gas volumes with high dust concentrations. However, in the case of incorporated ceramic monolith catalysts, where the active phase is homogeneously distributed throughout the solid and not just on the surface, the effective usage of catalytic active phase is sometimes inefficient due to internal mass transfer limitations [9].

This phenomenon may be reduced by diminishing either the particle size for pellets and cylinders in conventional shaped catalysts or the wall thickness of monolithic ones. For the latter case this method is limited by a severe loss in the mechanical strength. A different approach to avoid mass transfer limitations is to increase the porosity of the solids, favouring thus the accessibility of the reactants towards the active sites located within the monolith walls.

Recent studies concerning the synthesis of materials with controlled micro–meso–macropore structure, zeolite type or metal oxides such as alumina, silica, titania or zirconia [10–12] have shown great interest. For the generation of the meso–macropores, surfactants [13], starch [14], polystyrene (PS) beads [15] and mesoporous carbon have been used as templates during the synthesis process and subsequent elimination through different methods. Ordered mesoporous carbon as a mould for the synthesis of mesoporous ordered materials have been

* Corresponding author. Tel.: +34 91 585 48 80; fax: +34 91 585 47 60.
E-mail address: jblanco@icp.csic.es (J. Blanco).

0920-5861/$ – see front matter © 2005 Elsevier B.V. All rights reserved.
doi:10.1016/j.cattod.2005.06.019

studied by Schüth and coworkers [16–18]. The material precursors are impregnated into the pore system of the carbon-template, carbon is then eliminated in a combustion step while the prepared material retains its integrity. Nevertheless, these methods require a long time and a meticulous preparation that make them hardly applicable for the development of industrial catalysts for environmental solutions, where simplicity and process economy are key requirements.

Studies dealing with the preparation of ceramic supports displaying high porosity are not numerous. Yokota et al. developed a technique for preparing magnesium ceramic of high porosity, using spray freeze drying of aqueous magnesium sulphate solutions, where fine salt particles having open pores due to sublimation of ice crystal were produced [19]; highly porous magnesia was obtained by firing this green body, obtaining samples with bimodal pore size distributions of macropores in the micron range and mesopores smaller than 100 nm. Nevertheless, high temperatures up to 1300–1500 °C were required to obtain these materials. She et al. prepared high porosity silicon carbide (SiC) ceramics by oxidation-bonding process of a large amount of graphite incorporated into the SiC powder [20]; the pore diameter could be controlled by the particle size of graphite and/or SiC powders. High-porosity mullite advance ceramic material (ACM) with a pore structure in the micron scale was evaluated as a monolithic support for enzyme catalysed reactions [21]; the use of high porosity ACM monoliths lead to a more stable and more active structured bioreactor, compared to a classical cordierite ceramic monolith.

In the 1980s Blanco et al. patented ceramic monolithic catalysts based on vanadia supported on titania using α-sepiolite as a permanent additive for the SCR process [22,23]. Titanium oxide is an interesting material with multiple applications in catalysis and sepiolite (magnesium silicate) has been used as a permanent additive for ceramic monolith preparation [24–26]. The main role of sepiolite is to improve the rheological properties of the ceramic paste during the extrusion process and improve the porosity and mechanical strength of the heat-treated composite. No chemical interaction between the components of the support was detected and basically the main contribution of sepiolite was to improve the material textural properties. The optimization of the Al_2O_3/sepiolite ratio for the preparation of ceramic monolithic catalysts has been also recently reported [27].

In this article a new monolithic support, based on the improvement of the macroporosity, using activated carbon as a pore generating agent (PGA) added during the preparation of the ceramic dough with its subsequent elimination by thermal treatment was developed. A series of titania/magnesium silicate monolithic supports with different ratios were prepared. The influence of the increased porosity of vanadia based catalysts in the selective catalytic reduction of NO_x with ammonia as a test reaction was analysed. From this study it seems clear that activated carbon was a useful PGA to increase the macroporosity of the catalyst, yielding a narrow pore size distribution. An estimation of the effectiveness factor for catalysts with the enhanced physical properties was calculated, considering the two main pore size distributions of these bimodal catalyst supports.

2. Experimental part

2.1. Support and catalyst preparation

A range of titania/magnesium silicate monolithic supports with weight ratios of 7/3, 1/1 and 0/1, using TiO_2 anatase from Rhône-Poulenc and sepiolite from Tolsa S.A. were prepared (Table 1). These monoliths were manufactured by extrusion of doughs prepared by kneading titania, sepiolite as binder and water. To increase the porosity, 10 wt.% of activated carbon was added during the ceramic paste preparation process. The activated carbon (Chemviron Carbon) used as a PGA had a specific surface area S_{BET} 1165 $m^2\ g^{-1}$, pore volume 0.75 $cm^3\ g^{-1}$ and particle size 90% < 12.25 μm with a mean particle size around 4 μm. The monolithic green bodies prepared by extrusion were subsequently dried and heat-treated at 550 °C for 4 h in air, for phase transformation and carbon removal when necessary. The monolithic supports had the following geometric dimensions: square cell size 3.6 mm, wall thickness 0.9 mm, geometric surface 8.1 $cm^2\ cm^{-3}$ and cell

Table 1
Composition and textural properties of monolithic supports prepared with different titania/magnesium silicate ratios. Standard (Ti) and improved supports (Ti*) prepared with PGA

Sample	Composition (wt.%)			Surface area ($m^2\ g^{-1}$)	Pore volume (MIP)[a] ($cm^3\ g^{-1}$)	Mean pore diameter > 50 nm	C.S.[b] ($kg\ cm^{-2}$)
	TiO_2	Silicate	Carbon				
Ti_{70}	70	30	–	92	0.50	75	142
Ti^*_{70}	70	30	(10)	95	0.73	130	76
Ti_{50}	50	50	–	105	0.53	60	194
Ti^*_{50}	50	50	(10)	104	0.73	130	127
Ti_0	0	100	–	135	0.49	–	176
Ti^*_0	0	100	(10)	132	0.74	–	102

[a] MIP: mercury intrusion porosimetry.
[b] Crushing strength.

density 7.7 cell cm^{-2}. The support composition and textural properties of the monoliths are collated in Table 1.

Vanadia based catalysts with a V_2O_5 content of 5.5 wt.% were prepared by impregnation of the monolithic supports with aqueous solutions of vanadyl sulphate ($VOSO_4 \cdot 5\ H_2O$, Fluka 96%). After impregnation for 30 min, the systems were dried at room temperature for 24 h, then at 100 °C and finally treated at 550 °C in air for 4 h.

2.2. Characterisation techniques

Vanadium content was determined by inductively coupled plasma (ICP) optical emission spectroscopy (Perkin-Elmer Optima 3300 DV) of acid solutions of the ground catalysts. X-ray diffraction (XRD) patterns of powdered samples of the monolithic catalysts were recorded on a Seifert 3000 P diffractometer, using Cu $K\alpha_1$ radiation: $\lambda = 0.15406$ nm. TGA–DSC curves were measured on a Netzsch 409 EP Simultaneous Thermal Analysis device. Approximately 20–30 mg of powdered sample were heated in an air stream of 75 mL min^{-1} at a rate of 5 °C min^{-1} from ambient to 1000 °C, using α-alumina as reference. Surface areas were measured by nitrogen adsorption–desorption, using a Sorptomatic 1800. Samples were outgassed overnight at 300 °C to a vacuum of $<1.33 \times 10^{-2}$ Pa to ensure a dry clean surface, free from any loosely held adsorbed species. The porosity in pores from 300 μm down to 7.5 nm were determined by mercury intrusion porosimetry (MIP) using CE Instruments Pascal 140/240 porosimeter on samples previously dried overnight at 150 °C. Combination of the results from nitrogen adsorption–desorption and MIP lead to the determination of the total pore volume of the materials. The mechanical strength of the monoliths was determined with a Chantillon dinamometer model LTCM with a 1 mm diameter die head.

2.3. Catalytic activity tests

Activity measurements of the monolithic catalysts were carried out in a continuous tubular glass reactor, which operated at integral regimen close to an isothermal axial profile, described elsewhere [28]. The inlet and outlet NO and NO_2 concentrations were determined by chemiluminescence with a Signal NO + NO_2 analyser Series 4000. Analysis of NH_3 was carried out by FTIR spectroscopy with a A.D.C. Double Beam Luft Type Infra-red Gas Analyser. Evolution of the gas composition at the reactor outlet was recorder by a Yokowaga Model 436006 multichannel analogical-digital register. The concentration data were acquired at steady state conditions, approximately after 90 min of reaction at each temperature.

The operating conditions for the experiments were: gas hourly space velocity at normal conditions GHSV (NTP) = 10000 h^{-1}, linear velocity $v_L = 0.98$ m s^{-1}, pressure P = 120 kPa, temperature T = 180–350 °C. The gas inlet compositions was: $[NO_x]$ = 1000 ppm, $[NH_3]/[NO_x]$ = 0.8 or 1, $[O_2]$ = 4 vol.%, and $[N_2]$ = balance.

3. Results and discussions

A PGA used as a porous structure modifier should fulfil two main requirements: (i) it should not modify the chemical nature of the support and (ii) it should not alter the crystal phases during the decomposition process. In order to determine the optimum calcination temperature of the support, TGA–DSC analyses in an air atmosphere were conducted. The results obtained for the activated carbon alone, and the titania/magnesium silicate (1/1) prepared with a 10 wt.% of PGA (Ti^*_{50}) are depicted in Fig. 1a and b, respectively. The PGA started to decompose in an exothermic process at 450 °C, concluding at around 650 °C. At 600 °C 50% of the sample weight was lost, coinciding with the peak maximum in the DSC curve (Fig. 1a). With Ti^*_{50} two weight losses were observed (Fig. 1b): an initial weight loss in the 25–200 °C range ascribed to the elimination of physisorbed water from titania and sepiolite and a second weight loss between 400 and 670 °C due to decomposition of the PGA. The maximum in the exothermic peak, attributed to carbon decomposition, was attained around the same temperature as that of the PGA alone. The phase changes that the silicate binder undergoes during the heat treatment have been thoroughly studied [29,30]. After loosing adsorbed water up to 80–100 °C, at 300 °C the structure begins to fold in a step called rotation. At higher temperatures up to 600 °C all the coordination water molecules are lost and the structure undergoes a so-called distortion. At 827 °C the sepiolite transformation to enstatite takes place with a characteristic endothermic peak (DCS curve). Titania in the anatase form is

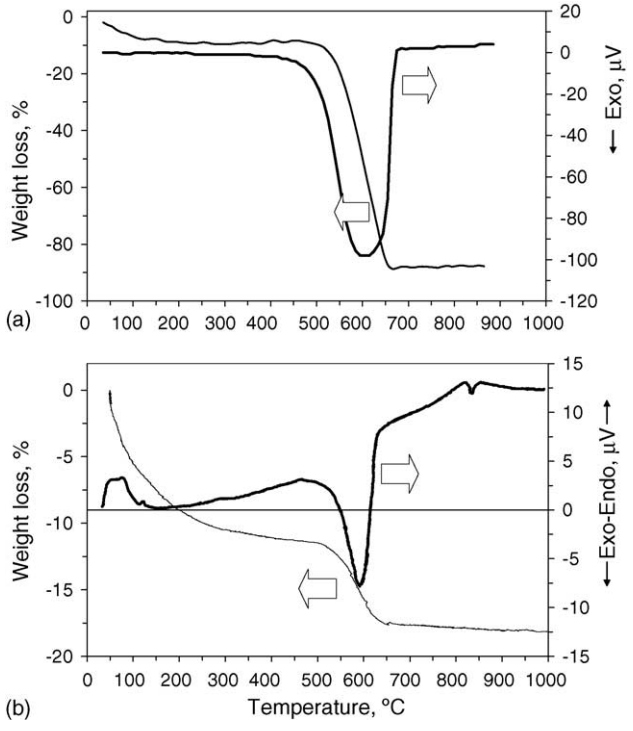

Fig. 1. TGA–DTA curves for: (a) PGA and (b) Ti^*_{50} fresh sample. Temperature range 25–1000 °C at a rate of 5 °C min^{-1}.

metastable and its transformation to rutile is thermodynamically favoured at temperatures above 600 °C [31], however, this phase transformation is retarded when intimately mixed with sepiolite [32]. The TGA–DSC curves obtained for supports prepared with different titania contents, (Ti^*_{70} and Ti^*_0 figures not shown) presented the same trend, losing the PGA in the same temperature range as the Ti^*_{50} sample. Even under dynamic conditions the weight loss ended at 650 °C, the TGA analysis performed at 550 °C during 4 h demonstrated the complete decomposition of the PGA under these conditions, which were subsequently chosen for the heat-treatment. In Fig. 2 a photograph of the ceramic monolith prepared with a 10 wt.% of PGA before and after calcination is shown. The ceramic paste prepared presented suitable rheological properties for extrusion, with an adequate viscosity and plasticity. The colour change from grey to white was evidence that the PGA had been completely decomposed during the heat-treatment at 550 °C in an air atmosphere. Samples with 15 and 20 wt.% of PGA were also prepared and analysed. Monoliths with very low mechanical strength were obtained, and the fragility of these supports made them not viable from an industrial point of view.

The XRD diffractograms for titania, and Ti_{50}, Ti^*_{50} samples are presented in Fig. 3. The titania sample showed the typical diffraction pattern of anatase phase with the most intense peak centred at 25.2° ($d = 3.52$) and the characteristic doublet at 53.9° ($d = 1.7$) and 55.1° ($d = 1.66$) ASTM 21-1272. The diffraction patterns of Ti_{50} and Ti^*_{50} only show the reflections of TiO_2-anatase and magnesium silicate (ASTM 26-1226) phases [33]. The results confirm that the elimination of the PGA caused no chemical changes to the support components.

The specific surface areas calculated by use of the BET equation from the nitrogen adsorption–desorption isotherms, pore volume and main pore diameters obtained by mercury intrusion porosimetry (MIP) are presented in

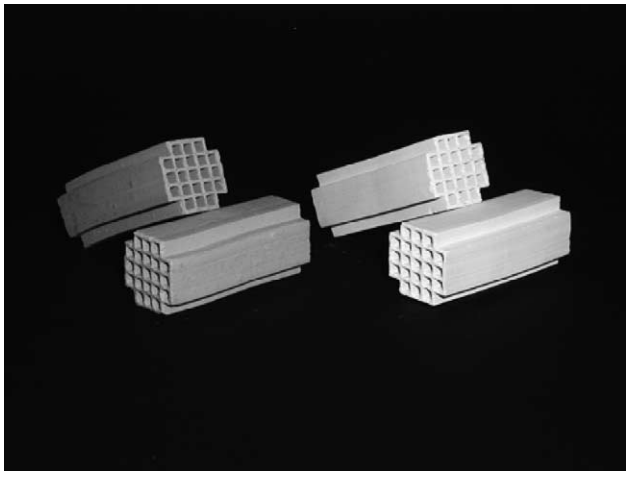

Fig. 2. Photograph of 21 cell monolithic supports prepared with a 10 wt.% of PGA before (left) and after (right) the heat-treatment process (550 °C for 4 h).

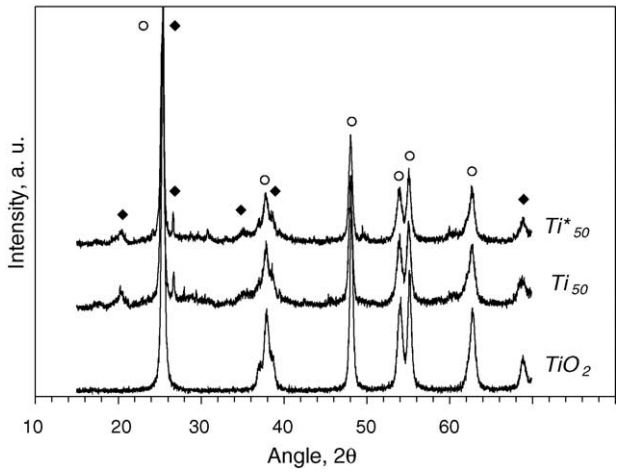

Fig. 3. X-ray pattern of titania and monolithic support prepared with/without PGA, treated at: 550 °C for 4 h, (○) TiO_2-anatase and (◆) magnesium silicate.

Table 1. The surface areas of the supports were very close to those calculated from the areas of the two components (135 and 75 $m^2\ g^{-1}$ for titania and sepiolite treated at 550 °C, respectively) indicating that under these conditions there was no interaction between the two components. As expected, the addition of the PGA did not modify these values, demonstrating that it was completely eliminated during the calcinations process without affecting the other permanent components. These results, together with the X-ray diffraction patterns of these supports (Fig. 3), indicated that no solid-state reactions occurred during mixing and heat-treating the PGA with titania and sepiolite. However, a considerable increase in the pore volume from around 0.50 to 0.74 $cm^3\ g^{-1}$ was produced, with a consequent decrease in the mechanical strength.

In Figs. 4 and 5 the MIP results are depicted as cumulative volume and differential intrusion as a function of the pore diameter for the samples described in Table 1. A clear increase of the total pore volume of around 40% was evident in all cases that PGA was incorporated in the support preparation and subsequently eliminated by heat treatment. The supports prepared with sepiolite (Figs 4a and 5b) presented the characteristic bimodal mesoporous structure of this material with pores around 20 and 40 nm diameter [34]. The enhancement in the volume of pores with diameters greater than 100 nm produced by the elimination of the PGA may be clearly observed. An additional macropore contribution appeared when TiO_2 was included with a typical pore diameter at 60 nm (Figs. 4b, c, 5b and c) due to the primary particle size of the titania raw material. The increase in titania content from 50 to 70 wt.% shifted the mean macropore diameter from 60 to 75 nm.

According to previous data obtained by SEM microscopy, titania was conformed as spherical particles of around 0.05–0.1 μm diameter that form aggregates of 0.3–1 μm where the original particles keep their identity [24]. The natural magnesium silicate used in this study has a fibrous

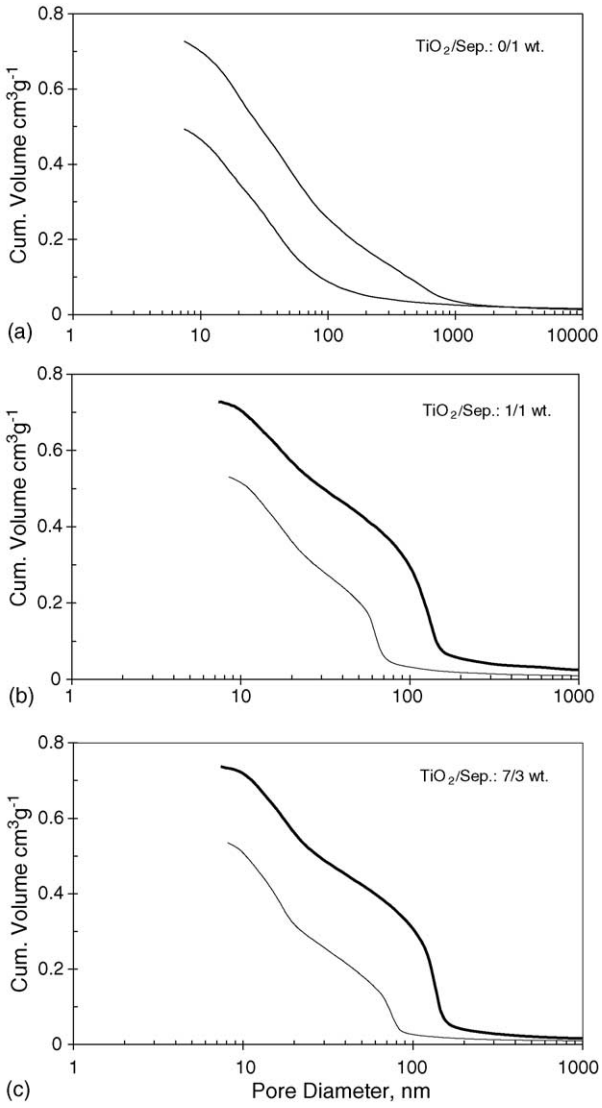

Fig. 4. Cumulative pore volume curves obtained by mercury intrusion porosimetry (MIP) of monolithic supports prepared with different TiO_2/sepiolite weight ratio: samples prepared without PGA (narrow line) and with PGA (thick line).

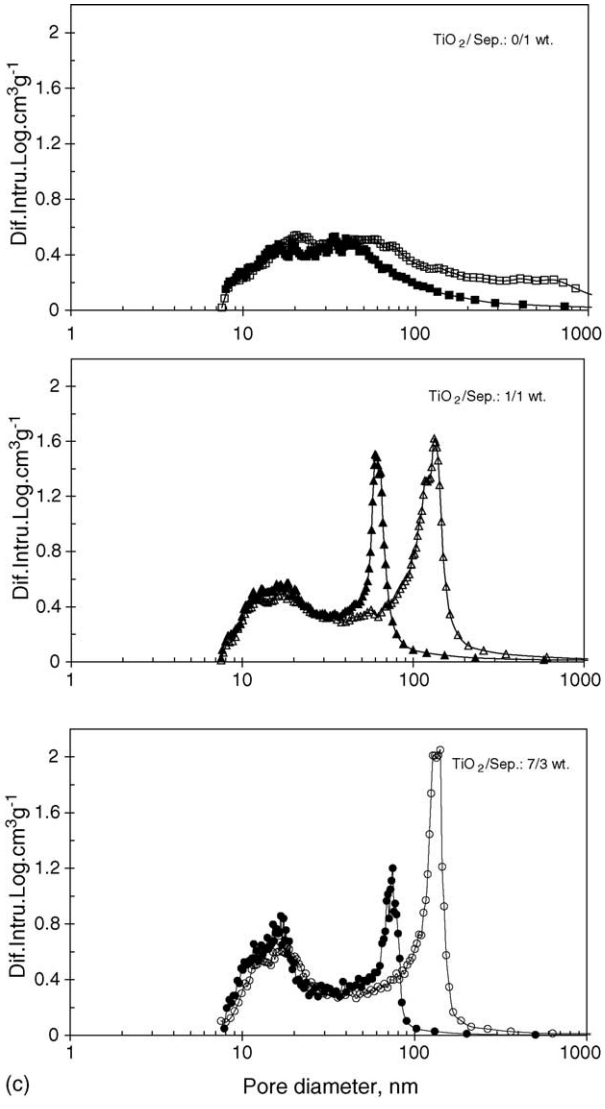

Fig. 5. Pore size distribution (PSD) of monolithic supports prepared with different TiO_2/sepiolite weight ratio: samples prepared without PGA (filled figures) and with PGA (empty figures).

structure ranging from 0.2 to 2.4 μm in length and 0.1–0.3 μm in diameter for the bundles of fibres [35]. These fibres act as a matrix were titania particles can be dispersed and stabilised. The inclusion of the PGA and subsequent heat-treatment produced a shift of these larger macropores from around 60 nm to about 130 nm but had no effect on the narrower pores. These results seem to indicate that the new contribution is related to the separation between titania particles/aggregates.

The effect of PGA incorporation on the ceramic composite is drawn in Fig. 6, considering the dimension of sepiolite bundles and titania aggregates. In the conventional preparation (Fig. 6a) the titania particle/aggregates are covered by sepiolite fibres. Nevertheless, when PGA is used in the preparation it is located between the titania spheres increasing the separation between them (Fig. 6b), and thus the interparticulate distances are enhanced. During the calcination process the PGA is decomposed, yielding large cavities that are accessed by these wider interparticulate pores. The diameter observed by MIP is a measure of these interparticulate distances.

The effect of the increased porosity on the catalytic activity was studied using the selective catalytic reduction (SCR) of NO_x with ammonia in excess oxygen as a test reaction. For this process vanadia/titania systems have shown excellent performances [36,37]. Thus, titania/sepiolite catalysts with a vanadia loading of 5.5 wt.% were prepared by impregnation, using supports with different titania/sepiolite ratios. In Fig. 7 the NO_x conversion and the ammonia slip curves for catalysts prepared with and without PGA are depicted. The catalytic tests were conducted using a gas feed composition of NO/NO_2, NH_3/NO_x of 0.8 at a gas hourly space velocity of

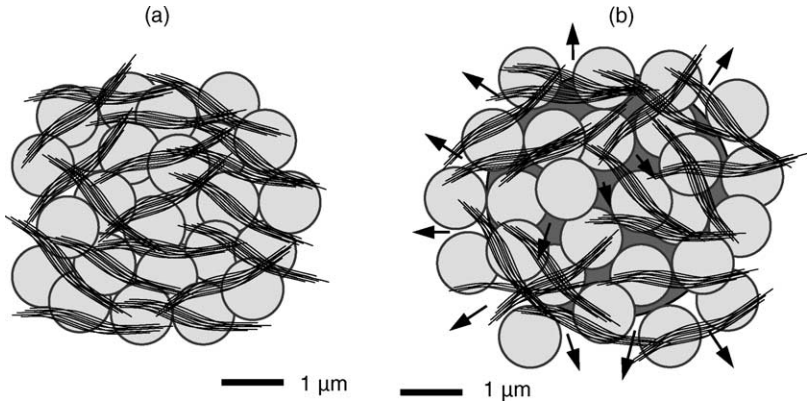

Fig. 6. Scheme of: (a) conventional monolithic support prepared without PGA and (b) with PGA. TiO_2 aggregates (grey spheres), sepiolite fibres (wavy lines) and the PGA (dark grey sphere).

10,000 h^{-1} and linear velocity of 1 m s^{-1} at 180 °C. The NH_3/NO_x ratio was selected to minimise the ammonia slip. Considering the reaction stoichiometry conversions higher than 80% cannot be achieved.

The results revealed a better performance towards the NO_x conversion for the high porosity Ti* materials compared with the analogous Ti samples, except for the case of sepiolite supports that were almost unchanged. Conversions close to 80% were achieved in the case of samples prepared with titania modified supports. Since the differences in the NO_x conversion between the $Ti*_{70}$ and the $Ti*_{50}$ samples were not significant and considering the mechanical strengths of the solids the $Ti*_{50}$ sample was selected for further studies. A different gas feed composition was chosen with a NH_3/NO ratio of 1 and using only NO as NO_x. The results are shown in Fig. 8 for catalysts $Ti_{50}V_5$ and $Ti*_{50}V_5$ in the temperature range between 180 and 350 °C. Again the same tendency was observed. The catalyst prepared with PGA displayed improved performance towards NO_x conversion compared to the conventional catalyst around 10–15 vol.%. Thus, $Ti*V_5$ presented a conversion of 85 vol.% at a temperature 30 °C lower that the TiV_5 and reached a maximum value of 97 vol.%

Since the surface area and active phase loading were similar for these two catalysts, the differences in their activities could only be explained by the change in their textural properties. The improved accessibility of the reactants to the active sites in the modified support, decreases any mass transfer limitations. This hypothesis was supported by estimation of the effectiveness factor.

3.1. Estimation of effectiveness factors

The internal effectiveness factors, η was estimated as a function of the Thiele modulus, ϕ, for a flat porous plate, supposing a first order reaction and isothermal conditions [38]. The combined diffusional coefficient was determined considering two pore size distributions, mesopores from 8 to 50 nm and macropores from 50 to 200 nm.

$$\eta = \frac{\tanh \phi}{\phi} \quad (1)$$

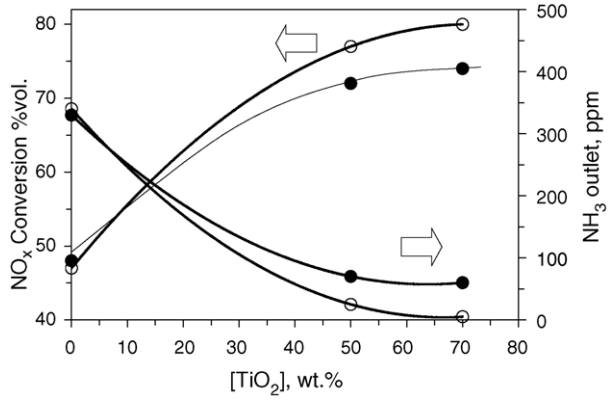

Fig. 7. NO_x conversion and ammonia slip as a function of the TiO_2 content for: (●) conventional TiV_5 and (○) modified $Ti*V_5$ monolithic catalysts. Feed composition: $[NO_x]$ = 1000 ppm, $[NO]/[NO_x]$ = 0.54, $[NH_3]/[NO_x]$ = 0.8, $[O_2]$ = 4 vol.%. Operating conditions: GHSV (NTP) = 10,000 h^{-1}, v_L = 0.98 Nm s^{-1}, T = 180 °C, P = 120 kPa.

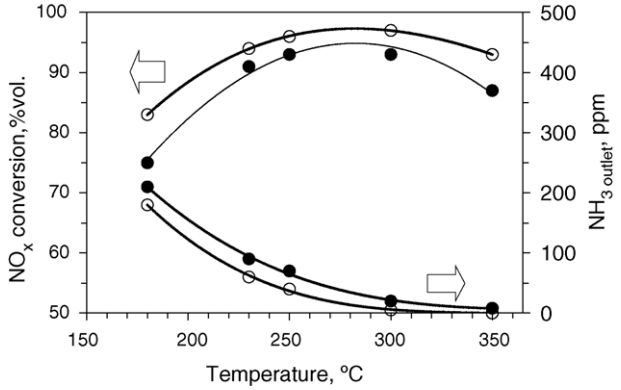

Fig. 8. NO conversion and ammonia slip as a function of temperature for conventional $Ti_{50}V_5$ and modified $Ti*_{50}V_5$ monolithic catalysts. Feed composition: $[NO_x]$ = 1000 ppm, $[NO]/[NO_x]$ = 1, $[NH_3]/[NO_x]$ = 1, $[O_2]$ = 4 vol.%. Operating conditions: GHSV (NTP) = 10,000 h^{-1}, v_L = 0.98 Nm s^{-1}, P = 120 kPa.

where the Thiele modulus, ϕ, is:

$$\phi = L\sqrt{\frac{k\rho_p}{D_e}} \quad (2)$$

where L is the characteristic length (half wall monolith thickness = 0.45 mm), k is the kinetic constant, ρ_p is the monolith density, and D_e is the effective diffusion coefficient.

The kinetic constant at 180 °C was estimated from the kinetic equation of the catalyst, obtained operating in differential regime [33]:

$$\log k = -2.504 \times 10^3 \frac{1}{T} + 15.46 \quad (3)$$

where T is the operating temperature. At T = 453 K (180 °C), the value of the kinetic constant was $k = 6.42\ \mathrm{cm^3\ g^{-1}\ s^{-1}}$. The monolith density, ρ_p, was estimated from mercury intrusion porosimetry results.

The effective diffusion coefficient, D_e, was estimated following Smith [39]:

$$D_e = \frac{D_c \varepsilon_p}{\tau} \quad (4)$$

where ε_p is the porosity of the catalyst, τ is the tortuosity factor, and D_c is the combined diffusion coefficient, defined as follows if there are more than one pore size contributions:

$$D_c = \sum \frac{V_i/V}{(1/D_{NO-N_2}) + (1/(D_K)_i)} \quad (5)$$

where D_{NO-N_2} is the molecular diffusion coefficient of nitrogen oxide in nitrogen, and $(D_K)_i$ is the Knudsen diffusion coefficient for the pores size contribution i. V_i is the pore volume of contribution i, and V is the total pore volume, both estimated from nitrogen adsorption–desorption and mercury intrusion porosimetry data.

The value of the tortuosity factor was considered to be $\tau = 4$, as indicated by Smith [39] for this type of porous ceramic material. D_{NO-N_2} was estimated by the Chapman–Enskog equation [40] employing the parameter published by Hirshfelder et al. [41]:

$$D_{NO/N_2} = 1.8583 \times 10^{-3} T^{3/2} \cdot \frac{[(1/M_{NO}) + (1/M_{N_2})]^{1/2}}{P_t \sigma^2_{NO/N_2}\, \Omega_{NO/N_2}} \quad (6)$$

where T is the temperature = 453 K (180 °C), P_t is the total pressure of the gas mixture P = 1.18 atm, M_{NO} and M_{N_2} are the molecular weights of nitrogen oxide and nitrogen, Ω_{NO/N_2} is the collision integral (0.870), which is a function of $k_B T/\varepsilon_{NO/N_2}$; σ_{NO/N_2} (3.575 Å) and ε_{NO/N_2} (1.440×10^{25} J) are parameters of the potential function of Lennard-Jones for the couple NO/N_2, and k_B is the Boltzman constant = $1.3805 \times 10^{23}\ \mathrm{J\ K^{-1}}$. In these conditions, a value of $D_{NO/N_2} = 0.357\ \mathrm{cm^2\ s^{-1}}$ was obtained. The Knudsen diffusion coefficient was estimated by assuming that the pores behave as cylinders with a mean radius $\bar{r}$:

$$(D_K)_i = 9.70 \times 10^3\, \bar{r}_i \sqrt{\frac{T}{M_{NO}}} \quad (7)$$

where $\bar{r}_i$ is the mean pore radius of the selected pore size range, determined by mercury intrusion porosimetry, T is the temperature in K, and M is the molecular weight of the diffusing molecule, NO.

The cumulative volume curves for catalysts conserved the characteristic shape of those of the support, with a slight decrease in the pore volume as a consequence of the deposition of the active phase. Taking into account the two main pore size contributions (8–50 nm, and 50–200 nm) the data collated in Table 2 allowed the estimation of the combined diffusion coefficient, D_c, for both catalysts using Eq. (5) (Table 3).

From these data, the effective diffusion coefficient (D_e, Eq. (3)), the Thiele modulus, (ϕ, Eq. (4)), and the effectiveness factor (η, Eq. (1)) were calculated. The results of the estimations for both catalysts are presented in Table 3 These results indicated that the enhancement in pores above 50 nm from 0.26 to 0.51 $\mathrm{cm^3\ g^{-1}}$ lead to an improvement in

Table 2
Porous structure data for vanadia catalysts supported on titania/sepiolite (1/1 wt.) monoliths prepared with and without PGA

Catalyst	Pore range (nm)	Mean radius $\bar{r}$ (nm)	$(D_K)_i$ ($\mathrm{cm^2\ s^{-1}}$)	V_p ($\mathrm{cm^3\ g^{-1}}$)	V_p/V
$Ti_{50}V_5$	8–50	20	0.075	0.22	0.47
	50–200	75	0.283	0.26	0.55
$Ti^*_{50}V_5$	8–50	20	0.240	0.11	0.18
	50–200	75	0.350	0.51	0.82

Table 3
Parameters and results of the effectiveness factor estimation at 180 °C for vanadia catalysts supported on titania/sepiolite (1/1 wt.) monoliths, prepared with and without PGA

Catalyst	ε_p	ρ_p ($\mathrm{g\ cm^{-3}}$)	D_c ($\mathrm{cm^2\ s^{-1}}$)	D_e ($\mathrm{cm^2\ s^{-1}}$)	ϕ	η
$Ti_{50}V_5$	0.62	1.30	0.116	0.018	0.973	0.77
$Ti^*_{50}V_5$	0.70	1.16	0.171	0.030	0.714	0.87

the effectiveness factor by around 13%. These results confirmed that the conventional monolithic catalysts suffered from internal mass transfer limitations that were greatly reduced by the use of high porosity supports prepared with 10 wt.% PGA.

4. Conclusions

The use of activated carbon as a pore generating agent (PGA) was demonstrated to be an effective technique for preparation of ceramic monolithic supports with an enhanced macropore structure. The main role of the PGA was to enlarge the inter-particular distance between the metal oxide particles, furthermore, a narrow pore size distribution was attained. The macropore diameter was intimately related to the particle size of both the metal oxide and PGA employed. The reduction in the mechanical strength with the PGA loading was obviously due to the increase in the interparticulate macropore volume. Thus, a 10 wt.% of PGA was chosen as the optimum amount to improve the porosity volume but preserve an adequate mechanical strength. The PGA chosen (activated carbon) acted exclusively as an inert compound since no chemical interactions with the other components of the support were observed.

The vanadia catalysts supported on these ceramic supports had better performances towards the low temperature NO_x elimination by the SCR process, than the conventional ones. An increase in the effectiveness factor by around 13% with respect to the catalyst prepared without PGA was estimated indicating that the mass transfer phenomena inside the porous ceramic structure was significantly improved.

Acknowledgements

The authors would gratefully acknowledge the CICYT (Projects MAT 2001-1597 and MAT 2000-0080-P4-02), and the Science and Technology Spanish Minister (I3P Program), for financial support.

References

[1] V. Stopka, Patente US 2.506. 244 (1950).
[2] L. Jhonson, W. Jhonson, D. O'Brien, Chem. Eng. Prog. 57 (1961).
[3] G.R. Smith, Patente US 3.948.611. (1963).
[4] H.C. Andersen, W. Green, P. Romeo, Engelhard Ind. Tech. Bull. I (1966) 100.
[5] R.M. Heck, R.J. Farrauto, Catalytic Air Pollution Control Commertial Technology, Van Nostrand Reinhold, New York, 1995 , pp. 19–27.
[6] S. Irandoust, B. Andersson, Catal. Rev. Sci. 30–3 (1988) 341.
[7] R.M. Deugh, F. Kapteign, J.A. Moulijn, Top. Catal. 26 (1–4) (2003) 29.
[8] S. Cimino, L. Lisi, R. Pirone, G. Russo, Ind. Eng. Chem. Res. 43 (21) (2004) 6670.
[9] A. Cybulsky, J.A. Moulijn (Eds.), Structurated Catalysts and Reactors, Marcell and Dekker, Inc., New York, 1998.
[10] Z-Y. Yuan, T-R. Ren, B-L. Sue, Adv. Mater. 15–17 (2003) 1462.
[11] S. Vaudreuil, M. Bousmina, S. Kaliaguine, L. Bonneviot, Micro. Meso. Mater. 44–45 (2001) 249.
[12] Z-Y. Yuan, A. Vantomme, A. Leonard, B-L. Sue, Chem. Commun. (2003) 1558.
[13] Z-Y. Yuan, T.Z. Ren, A. Vantomme, B-L. Sue, Chem. Commun. 16 (2004) 5096.
[14] B. Zang, S. A: Davis, S. Manm, Chem. Mater. 14 (2002) 1369.
[15] V. Valtchev, J. Mater. Chem. 12 (2002) 1914.
[16] M. Schwickardi, T. Johann, W. Schmidt, F. Schüth, Chem. Mater. 14 (2002) 3913.
[17] W-C. Li, A-H. Lu, C. Weidenthaler, F. Schüth, Chem. Mater. 16 (2004) 5676.
[18] A-H. Lu, W. Schmidt, B. Spliethoff, F. Schüth, Chem. Eur. J. 10 (2004) 6085.
[19] T. Yokova, Y. Takanata, T. Katsiyama, Y. Matsuda, Catal. Today 69 (2001) 11.
[20] J.H. She, T. Ohji, S. Kanzaki, J. Eur. Ceram. Soc. 24 (2003) 331.
[21] K. Lathouder, J. Bakkera, M.T. Kreutzer, F. Kapteijn, J.A. Moulijn, S.A. Wallin, Chem. Eng. Sci. 59 (2004) 2027.
[22] J. Blanco, P. Avila, C. Barthelemy, A. Bahamonde, C. Chacón, J.M. Ramos, Patente ES 2.010. 849 (1982).
[23] A. Bahamonde, C. Barthelemy, C. Chacón, J.M. Ramos, J. Blanco, P. Avila, Patente ES 2.009. 397 (1989).
[24] P. Avila, J. Blanco, A. Bahamonde, J.M. Palacios, C. Barthelemy, J. Mater. Sci. 28 (1993) 4113.
[25] J. Blanco, M. Yates, P. Avila, A. Bahamonde, J. Mater. Sci. 29 (1994) 5927.
[26] S. Suárez, C. Saiz, M. Yates, J.A. Martín, P. Avila, J. Blanco, Appl. Catal. B 55 (2005) 57.
[27] J. Blanco, P. Avila, S. Suárez, M. Yates, J.A. Martín, L. Marzo, C. Knapp, Chem. Eng. J. 97 (2004) 1.
[28] J. Blanco, P. Avila, S. Suárez, J.A. Martín, C. Knapp, Appl. Catal. B 28 (2000) 235.
[29] H. Nagata, S. Shimoda, T. Sudo, Clays Clay Miner. 22 (1974) 285–293.
[30] C. Serna, J.L. Ahlrichs, J.M. Serratosa, Clays Clay Miner. 23 (1975) 452–457.
[31] A. W. Czanderna, C.N. Ramachandra, J.M. Honig, Trans. Fasraday Soc. 54 (1958), 1069.
[32] J. Blanco, P. Avila, M. Yates, A. Bahamonde, Stud. Surf. Sci. Catal. (1995) 755.
[33] S. Suárez, Desarrollo de catalizadores SCR áltamente selectivos a nitrógeno para plantas de ácido nítrico, Ph.D. thesis, Universidad de Alcalá, Madrid, 2002.
[34] M. Yates, J. Blanco, M.A. Martin-Luengo, M.P. Martin, Micro. Meso. Mater. 65 (2003) 219.
[35] A. Alvarez, in: A. Singer, E. Galan (Eds.), Developments in Sedimentology, Elsevier, 1984.
[36] G. Busca, L. Lietti, G. Ramis, F. Berti, Appl. Catal. B 18 (1998) 1.
[37] V.I. Pârvulescu, P. Grange, B. Delmon, Catal. Today 46 (1998) 223.
[38] G.F. Froment, K.B. Bischoff, Chemical Reactor Analysis and Design, Wiley, 1990,, p. 157.
[39] J.M. Smith, Chemical Engineering Kinetics, third ed., Mc Graw-Hill, New York, 1981 (Chapter 9).
[40] E. Costa, G. Calleja, G. Ovejero, A. De Lucas, J. Aguado, M.A. Uguina, Ingeniería Química 2: Fenómenos de Transporte 1a Edición, Alhambra Universidad, Madrid, 1985, p. 170.
[41] J.O. Hirschfelder, C.F. Curtis, R.B. Bird (Eds.), Molecular Theory of Gases and Liquids, Jonh Wiley & Sons Inc., New York, 1954 , pp. 1110–1111.